THE JOURNAL OF PHYSICAL CHEMISTRY B

Article

pubs.acs.org/JPCB

2D Spectroscopy Study of Water-Soluble Chlorophyll-Binding Protein from *Lepidium virginicum*

Jan Alster,[†] Heiko Lokstein,[‡] Jakub Dostál,[†] Akira Uchida,[§] and Donatas Zigmantas*[,†]

[†]Department of Chemical Physics, Lund University, P.O. Box 124, SE-221-00 Lund, Sweden

[‡]Glasgow Biomedical Research Centre, Institute of Molecular, Cell and Systems Biology, University of Glasgow, 120 University Place, Glasgow G12 8TA, Scotland/U.K.

[§]Department of Biomolecular Science, Faculty of Science, Toho University, 2-2-1 Miyama, Funabashi, Chiba 274-8510, Japan

Supporting Information

ABSTRACT: Water-soluble chlorophyll-binding proteins (WSCPs) are interesting model systems for the study of pigment−pigment and pigment−protein interactions. While class IIa WSCP has been extensively studied by spectroscopic and theoretical methods, a comprehensive spectroscopic study of class IIb WSCP was lacking so far despite the fact that its structure was determined by X-ray crystallography. In this paper, results of two-dimensional electronic spectroscopy applied to the class IIb WSCP from *Lepidium virginicum* are presented. Global analysis of 2D data allowed determination of energy levels and excitation energy transfer pathways in the system. Some additional pathways, not present in class IIa WSCP, were observed. The data were interpreted in terms of a model comprising two interacting chlorophyll dimers. In addition, oscillatory signals were observed and identified as coherent beatings of vibrational origin.

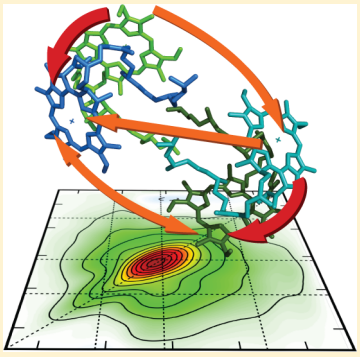

INTRODUCTION

Water-soluble chlorophyll-binding proteins (WSCPs) are a group of non-membrane-bound proteins found in some plant families.[1−3] Interestingly, WSCPs contain no carotenoids, unlike the vast majority of other chlorophyll (Chl)-binding proteins. Functions of WSCPs are not known with certainty, although sequestration, temporal storage, and/or transport of Chls and biosynthetic precursor molecules of Chl were suggested.[4−6] A direct participation of WSCPs in photosynthetic light-harvesting and energy conversion processes is not likely.[4−6] Two classes of WSCPs, occurring in different plant families, are known.[4] The two classes exhibit different photophysical properties: whereas class I WSCPs (e.g., from *Chenopodium album*) may undergo photoconversion upon illumination,[1] class II WSCPs (e.g., from *Brassica* species) are not photoconvertible. Class II WSCPs can be further subdivided into class IIa (e.g., from *Brassica oleracea* var. Botrys) and IIb (e.g., from *Lepidium (L.) virginicum*). The high resolution structure of class IIb WSCP from *L. virginicum* has been determined by X-ray crystallography[7] (Figure 1). The structure of this complex is tetrameric with each of the four apo-proteins binding one Chl molecule. The four Chls, enclosed and efficiently shielded from the environment in a hydrophobic cavity in the center of the complex, form two "open sandwich" dimers. The structure of class IIa WSCP is not known, although it is assumed to be very similar to the structure of class IIb. Interestingly, there are some significant differences between class IIa and class IIb WSCPs. Namely, the positions of the Q_y absorption band, comprised of the lowest transitions of individual Chls, differ considerably, 674 nm in IIa[2] vs 662 nm in IIb[3] at room temperature. Moreover, the two WSCP classes appear to have different contents of Chls per complex (two Chls on average for tetrameric reconstituted IIa vs four for native IIb).[7−9]

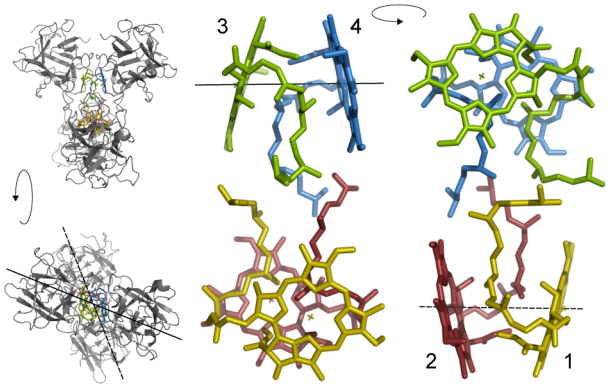

Figure 1. Structure of class IIb WSCP from *L. virginicum*.[7] (left) The pigment−protein complex in different orientations. (right) The central chromophore core comprising four Chl *a* molecules in two different orientations with individual sites marked with numbers. Note that in native WSCP some of the Chl *a* are substituted by Chl *b*. The figure was created from PDB file 2DRE using PyMOL.[10]

Received: November 13, 2013
Revised: March 14, 2014
Published: March 14, 2014

   dx.doi.org/10.1021/jp411174t | *J. Phys. Chem. B* 2014, 118, 3524−3531

Although WSCPs do not directly participate in photosynthesis, the content of very few structurally well ordered Chl molecules renders WSCPs ideal model systems for the study of pigment−pigment as well as pigment−protein interactions. Renger and co-workers have extensively studied recombinant class IIa WSCP from cauliflower, using a broad range of steady state and time-resolved spectroscopy techniques as well as theoretical calculations.[11] Class IIb WSCP, however, has attracted much less attention. Because of the presence of four Chls in WSCP type IIb, more complex interaction patterns between the pigments have to be expected, which can be readily studied by nonlinear time-resolved spectroscopic methods. In this paper, we present results of coherent two-dimensional electronic spectroscopy (2DES) applied to class IIb WSCP from *L. virginicum*. From the thus obtained data, the excitonic structure and excitation energy transfer pathways have been determined with the help of a global analysis.

MATERIAL AND METHODS

WSCP Isolation. Class IIb WSCP was isolated from Virginia pepperweed (*L. virginicum*) as described previously.[7] For 2DES measurements at 77 K, the sample was mixed with 68% (v/v) glycerol, to a final OD of 0.24 at the Q_y maximum.

Spectroscopy Setup. 2D spectra were obtained using the double-modulation lock-in technique described previously.[12] Briefly, a 200 kHz repetition rate, KGW amplified laser system (PHAROS, Light Conversion) was down-sampled to 2 kHz to prevent accumulation of long-lived (probably triplet) excited states in the sample and used to pump a homemade NOPA that produced broadband 15 fs (full width at half-maximum, fwhm, measured by autocorrelation) pulses centered at 656 nm with a spectral width (fwhm) of ∼50 nm. Using a plate beam splitter and a transmissive diffraction grating, the initial beam was split into four beams arranged in the boxcar geometry. One of the beams, the local oscillator, was attenuated by a 3 OD filter. The other three beams were used to excite the sample in a transient four-wave mixing arrangement. The excitation density at the sample was 1.7×10^{14} photons/(pulse cm^2). The first beam and the second beam were modulated at different frequencies, using optical choppers. Accurate time delays of the first two pulses were introduced by moving fused silica wedges with motorized translation stages. The delays and CCD detector were calibrated by using procedures outlined previously.[13] The signal, emitted from the sample in the phase-matched direction, was mixed with the collinear local oscillator beam and detected in a spectral interferometry scheme. Separation of the third-order signal from scattered light was performed by locking to the sum and difference of the chopper modulation frequencies. All measurements were done at 77 K, employing a Janis STVP-400 flow cryostat.

Interferometric detection allows determination of the amplitude and phase of the 2D signal; the real part of the total response, corresponding to a spectrally resolved transient absorption measurement, is shown in 2D spectra in this paper. The resolution of the originally collected data was 67 cm^{-1} on the excitation (ω_1) and 59 cm^{-1} on the detection axis (ω_3); however, 2D spectra as shown below were interpolated for better clarity.

RESULTS AND DISCUSSION

Linear Spectroscopy. WSCP can bind both Chl *a* and Chl *b* with their ratio depending on the growth conditions and plant tissue of origin.[4,14] The linear absorption spectrum of WSCP in the visible spectral region exhibits typical spectral features of Chl *a* and *b* (Figure 2). A band comprised of Q_y transitions of both Chls peaks at 663 nm. Multiple bands, Q_x transitions and vibrational progression of Q_y transitions of both Chls, can be observed in the region between 550 and 650 nm.[15,16] Soret bands of both Chls are observed at wavelengths shorter than 500 nm. Although spectral features of both Chls overlap, the distinctive band peaking at 470 nm is due to the Soret transition in Chl *b*.[3]

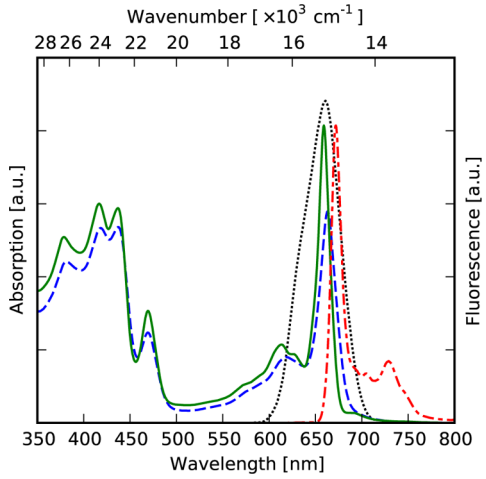

Figure 2. Low temperature (77 K, green solid line) and room temperature (300 K, blue dashed line) linear absorption spectra and low temperature fluorescence emission spectrum upon excitation at 415 nm (77 K, red dash-dotted line) of WSCP. The fluorescence maximum is normalized to the absorption maximum at 77 K. The black dotted line represents the spectrum of excitation laser pulses used in the 2DES experiments.

The absorption spectrum measured at 77 K exhibits narrower peaks and a slight blue shift of the Q_y band (to 659 nm) as compared to the room temperature absorption spectrum. Moreover, an additional weak band at ∼693 nm is resolved. A possible origin of this peak may be due to excitonic interaction(s). However, the observed splitting from the center of the Q_y band (∼700 cm^{-1}) would be much larger than expected for WSCP (cf. a splitting of ∼200 cm^{-1}, which was observed for reconstituted class IIa WSCP from cauliflower[15]). Moreover, as the lowest state of the excitonic manifold, this peak should receive all excitation energy, and fluorescence should emanate from this state. However, fluorescence was observed from a higher level (Figure 2), thus rendering the excitonic origin of the 693 nm peak unlikely. Another possible origin might be a Chl-like molecule (a precursor or catabolite) with red-shifted absorption of the Q_y band as compared to Chl *a*, which might be present in small amounts. However, such molecules (e.g., pheophytin) usually lack the central Mg ion and do not bind to WSCP.[9] The peak was not observed in the 2D spectra. This was most likely caused by the nonlinear nature of 2DES, which suppresses weak peaks relatively to stronger peaks, and prevents drawing any direct conclusions about the nature of this peak. Currently, we lack a credible interpretation of this peak. However, due to the fact that it is not observed in the 2DES measurements and it is disconnected from the other transitions, it does not play any role for interpretation of the data presented here. Individual peaks within the Q_y band are not well resolved; however, their positions can be approximately determined by second derivative analysis (Figure S1,

dx.doi.org/10.1021/jp411174t | J. Phys. Chem. B 2014, 118, 3524−3531

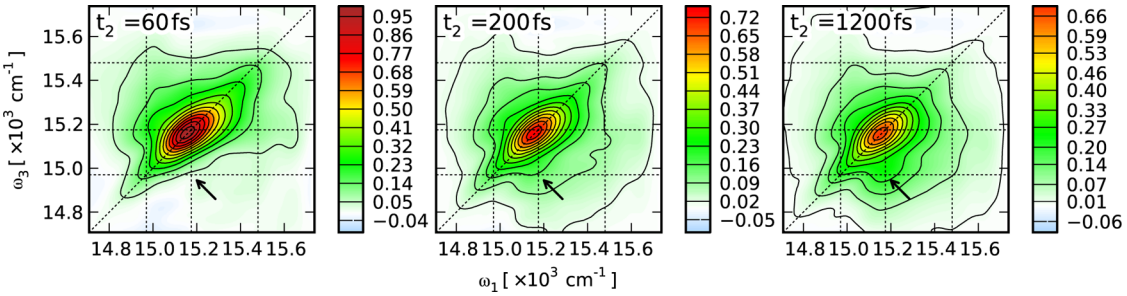

Figure 3. Evolution of the 2D spectrum of WSCP with increasing population time (t_2). The spectra were normalized to the maximum of the signal at t_2 = 60 fs. The guide lines indicate positions of the levels in the Q_y band determined by second derivative analysis of the linear absorption spectrum and the diagonal. The arrow marks the most prominent cross-peak, which indicates occurrence of excitation energy transfer.

Supporting Information): 646, 659, and 668 nm (15 480, 15 175, and 14 970 cm^{-1} respectively). These three peaks can be assigned to exciton levels on the basis of the analysis of the 2D spectra (see below).

The low temperature (77 K) fluorescence spectrum is shown in Figure 2. The maximum of the fluorescence is at 670 nm. The less pronounced peaks (to the red) correspond to transitions to vibrational levels of the ground state of Chl *a* (Figure S2, Supporting Information). The spectrum was measured upon excitation at 415 nm, where Chl *a* is predominantly excited. However, if Chl *b* is predominantly excited (at 470 nm), the fluorescence changes only very slightly, showing an ∼1 nm shift toward shorter wavelengths (Figure S2, Supporting Information). This indicates efficient excitation energy transfer from Chl *b* to Chl *a*, consistent with previous results.[17]

2DES. Typical 2D spectra of class IIb WSCP measured at 77 K at different population times (t_2) are shown in Figure 3. The spectra are dominated by ground-state bleaching (GSB) and stimulated emission (SE) signals and exhibit a complicated network of diagonal peaks and cross-peaks. The dominating feature is a strong central diagonal peak at $\omega_1 = \omega_3$ = 15 175 cm^{-1} (659 nm), corresponding to the absorption of the Q_y band. Weaker, overlapping cross-peaks appear above and (at later population times) below the diagonal. The broad positive signal above the diagonal, comprising several cross-peaks, indicates significant excitonic coupling between some of the Chls.

To illustrate this, vertical cuts obtained close to the red edge of the 2D spectrum at t_2 = 1200 fs are shown in Figure 4. These cuts correspond to the transient absorption spectra (with the convention of positive GSB) detected after excitation at the ω_1 frequency of the cut. Thus, only the states with the lowest energy were excited in cuts taken at the red edge of the 2D spectrum. However, clearly bleaching of higher states also appeared. This is only possible if the higher states share a common ground state with the lower (excited) state.

The ground state is shared for all electronic states of a single molecule and their vibrational progressions. Note, however, that the left-most peak in Figure 4 shifts with excitation frequency (i.e., excitation selects subpopulations of an inhomogeneously broadened transition), whereas the central peak is stationary and, therefore, cannot be part of the vibrational progression of the left peak. Moreover, the energy separation of the peaks (∼200 cm^{-1}) is much smaller than the separation of the two lowest electronic states of Chl (700 cm^{-1} or more[16]). Thus, the involved states cannot belong to a single molecule and have to be excitonic states of multiple,

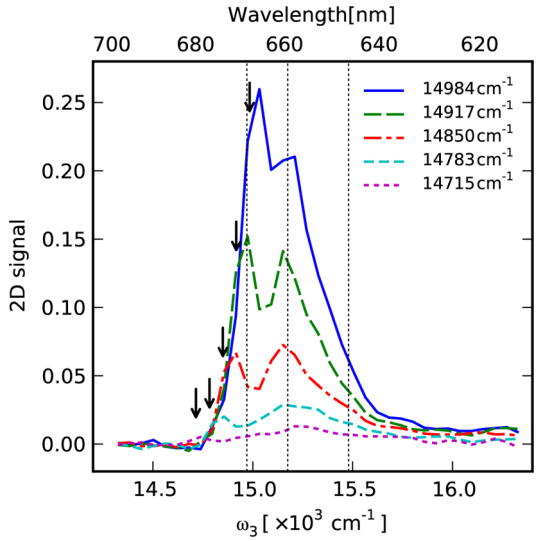

Figure 4. Cuts in the red edge of the excitation frequency of the (uninterpolated) 2D spectrum at t_2 = 1200 fs (Figure 3). The cuts correspond to transient absorption-like signals after excitation at the ω_1 frequency (which is given in the legend and marked by arrows). Vertical lines indicate positions of the levels in the Q_y band determined by second derivative analysis of the linear absorption spectrum.

excitonically coupled molecules. This does not exclude the possibility that part of the observed bleaching is due to a vibrational progression.

Analogous cross-peaks appear also below the diagonal. At early population times, the below-diagonal cross-peaks are masked by excited state absorption from the higher exciton state.

We performed a calculation on the basis of a simple point dipole approximation using the pigment positions from the high resolution structure (for details, see the Supporting Information). The calculation shows that, unsurprisingly, the strongest excitonic interaction is between the molecules in the two "open sandwich" dimers (sites 1−2 and 3−4 in Figure 1). Other couplings are much weaker, amounting to ∼20% of the strongest coupling between "vertically adjacent" sites 1−4 and 2−3 and ∼8% between "diagonal" sites 1−3 and 2−4, respectively. Consequently, we can consider the system as consisting of two dimers which are only weakly coupled to each other.

2D Global Analysis. Data measured for very early population times during the overlap of excitation pulses (t_2 < 50 fs) were found to be "contaminated" by nonresonant signals originating from interaction of the pulses with sample solvent

dx.doi.org/10.1021/jp411174t | J. Phys. Chem. B 2014, 118, 3524−3531

and cuvette walls and were omitted from the analysis. The analyzed data set consisted of 2D spectra measured for population times from 60 to 1200 fs, in 20 fs steps. Kinetics of selected diagonal peaks and cross-peaks are shown in Figure 5. The most prominent cross-peak (marked by an arrow in Figure 3) at ω_1 = 15 175 cm^{-1} (659 nm), ω_3 = 14 970 cm^{-1} (668 nm) appears below the diagonal peak at $\omega_1 = \omega_3$ = 15 175 cm^{-1} (659 nm). Kinetic traces associated with those peaks (solid blue and dashed green lines in Figure 5) reveal excitation energy transfer from the 15 175 cm^{-1} (659 nm) level to the 14 970 cm^{-1} (668 nm) level on a sub-100 fs time scale. Other dynamic processes are less evident; however, at least two other lifetimes can be discerned. Additionally, weak oscillating signals (approximately 5% of the maximum amplitude) can be observed in various regions of the 2D spectra and will be discussed below.

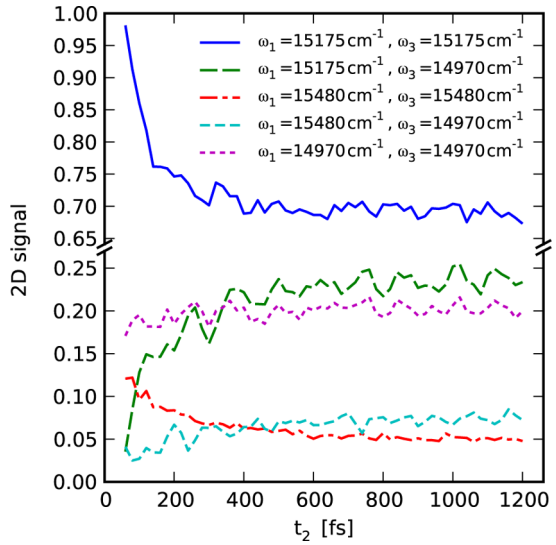

Figure 5. Evolution of the 2D signal with population time at main diagonal peaks and subdiagonal cross-peaks. Note that the visible oscillations are due to coherent beatings, not noise.

A simplified global analysis[18,19] (with oscillating signals not included in the model) was used to unravel population relaxation, resulting in a 2D version of the decay associated spectra (DAS). The global analysis reveals two components with lifetimes of ∼50 fs, ∼250 fs and a component with a lifetime much longer than the scanned population times, ≫1 ps (Figure 6).

The shortest lifetime resolved by global analysis, 50 fs, corresponds well to the previously calculated lifetime of the exciton relaxation in homodimers of Chl *a* in class IIa WSCP,[11] 50−80 fs. Indeed, the shape of the DAS also suggests excitation energy transfer from the state at ∼15 175 cm^{-1} (659 nm) to the one at ∼14 970 cm^{-1} (668 nm). The second component (250 fs) is markedly weaker (note the color scales in Figure 6) and contains characteristic features of multiple excitation energy transfer processes. The longest component can be assigned to the relaxation from the lowest state of the excitonic manifold to the ground state, which for class IIb WSCP at room temperature has a lifetime of 3.6 ns[17] and for class IIa WSCP at 10 K has a lifetime of 6−7 ns.[20] Note that we cannot determine such a long lifetime with the used apparatus. The repetition rate of 2 kHz had to be used in the current experiments to prevent accumulation of long-lived (triplet) species in the sample. The triplet states have typical lifetimes on the order of a few ms.[21] Thus, some part of the signal could be decaying on the corresponding time scale.

On the basis of the analysis of DAS, we propose a tentative model of excitonic levels and excitation energy transfer in the class IIb WSCP. In the following subsections, we present the global modeling of the 2D spectral shapes and population dynamics as well as examination of the coherent dynamics with the help of Fourier-transform analysis.

Modeling of DAS. To gain insight into the relaxation processes in WSCPs, we have created a simple, qualitative model and calculated associated DAS (see Figure 6). The modeling is somewhat complicated by the fact that the Chl *a* and Chl *b* occupancy in each of the individual WSCP complexes is not known. Most likely the sample consists of a mixture of complexes with different occupancies of the binding sites with Chl *a* and *b*. In the model, we assume that all four

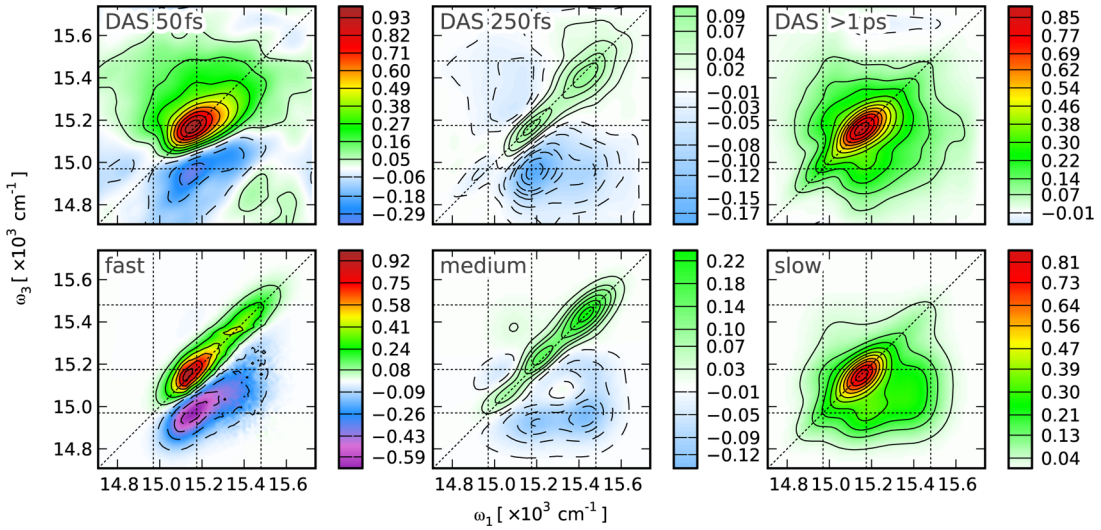

Figure 6. Decay associated spectra, as revealed by the global analysis of the experimental data (top row, normalized to the maximum of the 50 fs spectrum), compared to analogous calculated spectra (bottom row, normalized to the maximum of the "fast" spectrum). The calculation was based on the model of interacting dimers. The guide lines indicate positions of the sublevels in the Q_y band and the diagonal. See text for details.

dx.doi.org/10.1021/jp411174t | J. Phys. Chem. B 2014, 118, 3524−3531

Chl-binding sites in the tetrameric complex have the same affinity for Chl *a* or Chl *b*, and that differences between binding sites are negligible. By comparing the absorption spectrum of our sample with spectra published previously,[3] we can estimate the Chl *a* to Chl *b* ratio of our sample as ~2.4:1. Under these assumptions, we consider the sample as a mixture of complexes with different pigment compositions (sites 1,2:3,4): AA:AA (25%), AA:AB (41%), AB:AB (17%), AA:BB (9%), AB:BB (7%), and BB:BB (1%), where A and B stand for Chl *a* and Chl *b*, respectively.

Inhomogeneous broadening was simulated as independent fluctuations of site energies. Since the relative order of individual levels on the energy scale can change for some realization of site energies, the direction of energy flow between dimers is ambiguous and had to be determined for each realization of the site energies independently. However, relaxation rates were not calculated on a case-by-case basis. Effective excited state lifetimes were assumed instead: short lifetimes were assumed for exciton relaxation in dimers, somewhat longer ones for excitation energy transfer between dimers, and very long ones for relaxation from the lowest excited state to the ground state. Lifetimes determined by the global analysis, 50 and 250 fs, were used for "fast" and "medium" lifetimes, respectively. A lifetime of 10 ps was used as the "slow" lifetime; the model is not very sensitive to this value as long as it is much larger than 1 ps.

Each excited state of each possible complex gives rise to a contribution with a corresponding lifetime. Individual contributions were weighted by the relative occurrence of the complexes they originate from and sorted into a "fast", "medium", or "slow" DAS (Figure 6). To test the idea of two weakly coupled dimers in WSCPs, suggested by interpigment coupling strengths as inferred from the structure, a model without interdimer excitation energy transfer was tested but could not explain the experimental data. Therefore, interdimer energy transfer pathways were included. The resulting model is depicted in Figure 7. For more details about the model, see the Supporting Information. The model successfully reproduces

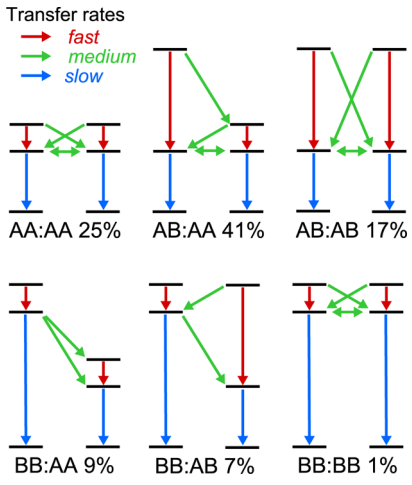

Figure 7. Schematic representation of the model of excited states and excitation energy transfer pathways in WSCP. The system is a mixture of complexes with different Chl *a* and Chl *b* compositions (A and B, respectively, with indicated probability of occurrence). Each complex is formed by two dimers. Each dimer is formed by a pair of excitonically coupled Chls. Relatively weaker interaction and energy transfer occurs between the two dimers. See text for details.

major spectral and dynamic features of the experimental data, supporting the idea of interdimer excitation energy transfer. In particular, it can explain the presence of multiple peaks in 250 fs DAS (compare experimental and calculated DAS in Figure 6).

The model predicts that six levels should be present in the system, two for each Chl *a* homodimer (AA), Chl *b* homodimer (BB), and Chl *a*−Chl *b* heterodimer (AB). However, only three distinct bands are observed in the experimental data. This is mainly due to the fact that inhomogeneously broadened spectral bands overlap and cannot be distinguished even with spectral narrowing at low temperature (77 K). Another reason is that BB homodimers occur with a low probability, with corresponding diminishing of its spectral features. The experimentally observed bands and the exciton states from the model can be assigned as follows: the 15 480 cm^{-1} (646 nm) band is due to the higher state of AB (15 380 cm^{-1}) and both states of BB (15 440 cm^{-1}, 15 260 cm^{-1}), the 15 175 cm^{-1} (659 nm) band is due to the higher state of AA (15 170 cm^{-1}), and the 14 970 cm^{-1} (668 nm) band is due to lower states of AA (14 970 cm^{-1}) and AB (15 050 cm^{-1}).

Note that Renger et al.[11] assigned a lifetime of 400 fs to the relaxation within an AB heterodimer. However, our model requires that exciton relaxations in all dimers are "fast". Using a lifetime of 400 fs for AB relaxation would lead to inclusion of several additional contributions to the "medium" DAS and, consequently, to changes incompatible with experimentally observed behavior. Therefore, we conclude that the exciton relaxation in the AB heterodimer is faster than 250 fs in class IIb WSCP.

Some details of the modeled DAS are apparently inaccurate. More specifically, the peaks in the 50 fs DAS are broader in the experimental data, suggesting that a more appropriate line shape should be used and/or a vibrational progression should be included in the model (compare with Figure 4). Another possibility might be that interactions between the dimers are strong enough so that these cannot be considered independent and each complex should be treated as an excitonic tetramer, with a corresponding spread of GSB signals. Additionally, the relative amplitudes of individual peaks are not always quantitatively reproducible; these depend strongly on energy transfer rate constants and on transient dipole moments, which were just estimated in our model.

Coherent Beatings. In recent years, coherent phenomena have attracted a lot of attention—especially with regard to 2DES of photosynthetic light-harvesting and reaction center complexes. The observation of oscillatory features (dynamical coherences) in 2D data of such systems was generally interpreted in terms of electronic coherences. Moreover, it was speculated that natural systems utilize quantum mechanical effects (i.e., coherent transfer of delocalized excitations) to enhance the efficiency of photosynthetic light harvesting.[22,23] In the current study, long-lived oscillations were observed for WSCP, which certainly does not function as a light-harvesting complex.

Residues remaining after subtraction of the population evolution (as three exponential decays) from the experimental data clearly exhibit oscillations, indicating the presence of coherent beatings. Frequencies of the oscillations (ω) can be determined by Fourier-transform analysis of the residues along the population time. Plotting the amplitude of a particular frequency in each point of the 2D spectrum results in an oscillation map of this frequency. The oscillation maps of two

dx.doi.org/10.1021/jp411174t | J. Phys. Chem. B 2014, 118, 3524−3531

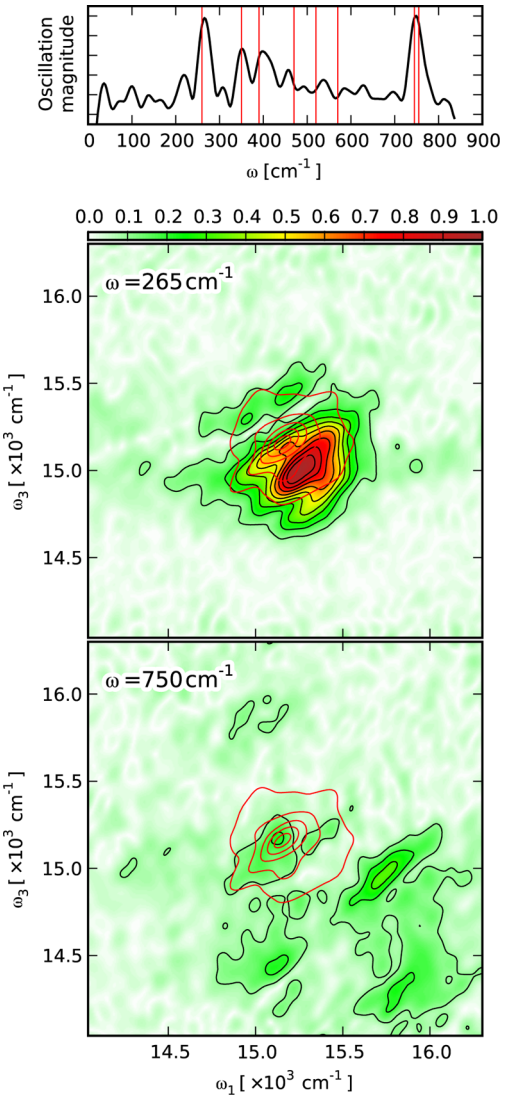

Figure 8. (top) Magnitude of observed coherent beatings. Vertical red lines indicate strong ground state vibrational frequencies of Chl *a*. (bottom) Rephasing part of the oscillation maps for the two strongest beatings, 265 and 750 cm^{-1} (normalized to the maximum of the 265 cm^{-1} oscillation map). An oscillation map shows parts of the 2D spectrum, where coherent beatings of a particular frequency are observed. The amplitude of the peaks in an oscillation map correspond to the amplitude of the beatings. Red contour lines depict the position of the 2D signal at t_2 = 1200 fs.

dominant frequencies (ω = 265 cm^{-1}, ω = 750 cm^{-1}) are shown in Figure 8, bottom. By integrating the corresponding oscillation map, the magnitude of the oscillation is obtained (Figure 8, top, and Table S2, Supporting Information). 2D oscillation maps have been shown to be very helpful for determining the origin of the coherent oscillations.[24−26]

To investigate the origin of the observed oscillations, we first consider the possible occurrence of electronic coherences. Such coherences would occur between excitonic levels, and the frequencies of the observed oscillations would match the energy gaps between these levels. Our model predicts energy gaps of ∼180, ∼200, and ∼330 cm^{-1} for individual excitonic dimers. Given the qualitative character of the model, some of the observed oscillations (∼200, ∼265, ∼350 cm^{-1}, see Figure 8, top) can be considered to match these energy gaps. However, dynamic electronic coherences would produce oscillation maps with the rephasing part consisting of two peaks, one above and another one below the diagonal, which were not observed in the current study. On the contrary, all strong oscillations produce rephasing oscillation maps with a five-peak structure (Figure 8), which is typical for vibrational coherence signals.[24] A missing (upper-right) peak would require an interaction at >16 470 cm^{-1}, which is outside of the spectral range covered by the used laser spectrum. Moreover, the determined frequencies are in good agreement with published vibrational frequencies of Chl *a*[27] (Figure 8, top, and Table S2, Supporting Information) and of class IIa WSCP[28] (Table S2, Supporting Information, see also below). Therefore, a contribution of electronic coherences to the observed signals is unlikely.

Vibronic or "mixed" type coherences[29−31] cannot be completely ruled out, because they produce similar oscillation maps to those caused by purely vibrational coherences.[31] However, judging by the small amplitude of the oscillatory signals, as discussed above, we do not observe substantial vibronic enhancement of the vibrational coherence signals.[32] Hence, it can be concluded that vibronic contributions can be only marginal. Thus, a vibrational origin is attributed to all dynamical coherences observed in the current 2D experiments on WSCP. In fact, in any biological complex containing pigments with nonzero coupling between electronic and vibrational transitions, vibrational coherence beatings will be observed.

Although it allows determination of vibrational frequencies in this manner, 2DES does not achieve the sensitivity or the resolution of more dedicated techniques. For example, the frequencies determined here match equally well (within experimental error) to vibrational frequencies of class IIa WSCP reconstituted with either Chl *a* or Chl *b*.[28] The 265 cm^{-1} mode seems to be stronger in class IIb than in IIa WSCP. Due to the low resolution, it is impossible to determine directly from the comparison of determined and previously published vibrational frequencies[28,33] (Table S2, Supporting Information) whether the coherences are on the ground state or on the excited state. However, it is expected that mostly ground state vibrational wavepackets contribute to the oscillating signals, because excited states should quickly dephase along energy relaxation and energy transfer in WSCP. Note that we have excluded data for t_2 < 50 fs from the analysis and therefore did not consider any signals (including possible excited state vibrational or electronic coherences) from this short time period.

In conclusion, we show that class IIb WSCP from *L. virginicum* shares many spectroscopic and dynamic properties with class IIa WSCP. However, it also exhibits additional excitation energy transfer pathways that were not observed for class IIa WSCP, mainly due to the presence of four Chls per tetrameric complex. WSCP complexes from different plants thus cover a broad range of pigment−pigment interaction patterns, from weakly coupled monomers and strongly coupled dimers[11] to interacting dimer pairs (or, possibly, even excitonically coupled tetramers). As such, they represent very good model systems for the study of pigment−pigment interactions of different coupling strengths. We did not observe any significant, long-lived dynamic electronic coherences and therefore conclude that WSCPs cannot be used as a model system in this regard. On the other hand, vibrational coherences were clearly visible. The comprehensive spectroscopic data in the current study were obtained on the same system for which a high-resolution structure has been

dx.doi.org/10.1021/jp411174t | J. Phys. Chem. B 2014, 118, 3524−3531

determined.[7] Determination of the full third order response of a pigment−protein complex with known high resolution structure forms an ideal basis for more detailed theoretical investigations.

■ ASSOCIATED CONTENT

Supporting Information

Second derivative analysis of low temperature absorption and fluorescence spectra. Calculation of pigment−pigment interactions. Technical details about the model used for calculation of DAS. A summary of vibrational frequencies of Chl *a*. This material is available free of charge via the Internet at http://pubs.acs.org.

■ AUTHOR INFORMATION

Corresponding Author

*E-mail: donatas.zigmantas@chemphys.lu.se.

Notes

The authors declare no competing financial interest.

■ ACKNOWLEDGMENTS

The authors thank Karel Žídek for his help with conducting the experiments. The group in Lund University gratefully acknowledges the financial support of Swedish Research Council and the Knut and Alice Wallenberg Foundation. The WSCP project was supported by LASERLAB-EUROPE (project LLC001692). H.L. acknowledges financial support from the BBSRC/EuroCore (BB/J00823011).

■ REFERENCES

(1) Yakushiji, E.; Uchino, K.; Sugimura, Y.; Shiratori, I.; Takamiya, F. Isolation of Water-Soluble Chlorophyll Protein from the Leaves of Chenopodium Album. *Biochim. Biophys. Acta* **1963**, *75*, 293−298.

(2) Murata, T.; Toda, F.; Uchino, K.; Yakushiji, E. Water-Soluble Chlorophyll Protein of Brassica Oleracea Var. Botrys (Cauliflower). *Biochim. Biophys. Acta, Bioenerg.* **1971**, *245*, 208−215.

(3) Murata, T.; Ishikawa, C. Chemical, Physicochemical and Spectrophotometric Properties of Crystalline Chlorophyll-protein Complexes from *Lepidium virginicum* L. *Biochim. Biophys. Acta, Bioenerg.* **1981**, *635*, 341−347.

(4) Satoh, H.; Uchida, A.; Nakayama, K.; Okada, M. Water-Soluble Chlorophyll Protein in Brassicaceae Plants is a Stress-Induced Chlorophyll-Binding Protein. *Plant Cell Physiol.* **2001**, *42*, 906−911.

(5) Damaraju, S.; Schlede, S.; Eckhardt, U.; Lokstein, H.; Grimm, B. Functions of the Water Soluble Chlorophyll-binding Protein in Plants. *J. Plant Physiol.* **2011**, *168*, 1444−1451.

(6) Bektas, I.; Fellenberg, C.; Paulsen, H. Water-Soluble Chlorophyll Protein (WSCP) of Arabidopsis Is Expressed in the Gynoecium and Developing Silique. *Planta* **2012**, *236*, 251−259.

(7) Horigome, D.; Satoh, H.; Itoh, N.; Mitsunaga, K.; Oonishi, I.; Nakagawa, A.; Uchida, A. Structural Mechanism and Photoprotective Function of Water-soluble Chlorophyll-binding Protein. *J. Biol. Chem.* **2007**, *282*, 6525−6531.

(8) Satoh, H.; Nakayama, K.; Okada, M. Molecular Cloning and Functional Expression of a Water-soluble Chlorophyll Protein, a Putative Carrier of Chlorophyll Molecules in Cauliflower. *J. Biol. Chem.* **1998**, *273*, 30568−30575.

(9) Schmidt, K.; Fufezan, C.; Krieger-Liszkay, A.; Satoh, H.; Paulsen, H. Recombinant Water-Soluble Chlorophyll Protein from *Brassica oleracea* Var. Botrys Binds Various Chlorophyll Derivatives. *Biochemistry* **2003**, *42*, 7427−7433.

(10) Schrödinger, L. L. C.

(11) Renger, G.; Pieper, J.; Theiss, C.; Trostmann, I.; Paulsen, H.; Renger, T.; Eichler, H. J.; Schmitt, F. J. Water Soluble Chlorophyll Binding Protein of Higher Plants: A Most Suitable Model System for Basic Analyses of Pigment−pigment and Pigment−protein Interactions in Chlorophyll Protein Complexes. *J. Plant Physiol.* **2011**, *168*, 1462−1472.

(12) Augulis, R.; Zigmantas, D. Two-dimensional Electronic Spectroscopy with Double Modulation Lock-in Detection: Enhancement of Sensitivity and Noise Resistance. *Opt. Express* **2011**, *19*, 13126−13133.

(13) Augulis, R.; Zigmantas, D. Detector and Dispersive Delay Calibration Issues in Broadband 2D Electronic Spectroscopy. *J. Opt. Soc. Am. B* **2013**, *30*, 1770−1774.

(14) Itoh, R.; Itoh, S.; Sugawa, M.; Oishi, O.; Tabata, K.; Okada, M.; Nishimura, M.; Yakushiji, E. Isolation of Crystalline Water-soluble Chlorophyll Proteins with Different Chlorophyll a and b Contents from Stems and Leaves of *Lepidium virginicum*. *Plant Cell Physiol.* **1982**, *23*, 557−560.

(15) Hughes, J. L.; Razeghifard, R.; Logue, M.; Oakley, A.; Wydrzynski, T.; Krausz, E. Magneto-Optic Spectroscopy of a Protein Tetramer Binding Two Exciton-Coupled Chlorophylls. *J. Am. Chem. Soc.* **2006**, *128*, 3649−3658.

(16) Reimers, J. R.; Cai, Z.-L.; Kobayashi, R.; Rätsep, M.; Freiberg, A.; Krausz, E. Assignment of the Q-Bands of the Chlorophylls: Coherence Loss via Qx - Qy Mixing. *Sci. Rep.* **2013**, *3*, No. 2761.

(17) Tabata, K.; Itoh, S.; Sugawa, M.; Nishimura, M. Effect of Sodium Dodecyl Sulfate on Structure and Spectroscopic Characteristics of Water-Soluble Chlorophyll Protein Complex Isolated from Stems of *Lepidium virginicum*. *Plant Cell Physiol.* **1983**, *24*, 987−994.

(18) Mullen, K. M. Separable Nonlinear Models: Theory, Implementation and Applications in Physics and Chemistry. Ph.D. thesis, Vrije University, Amsterdam, The Netherlands, 2008.

(19) van Stokkum, I. H. M.; Larsen, D. S.; van Grondelle, R. Global and Target Analysis of Time-resolved Spectra. *Biochim. Biophys. Acta, Bioenerg.* **2004**, *1657*, 82−104.

(20) Schmitt, F. J.; Trostmann, I.; Theiss, C.; Pieper, J.; Renger, T.; Fuesers, J.; Hubrich, E. H.; Paulsen, H.; Eichler, H. J.; Renger, G. Excited State Dynamics in Recombinant Water-Soluble Chlorophyll Proteins (WSCP) from Cauliflower Investigated by Transient Fluorescence Spectroscopy. *J. Phys. Chem. B* **2008**, *112*, 13951−13961.

(21) Angerhofer, A. In *Chlorophylls*; Scheer, H., Ed.; CRC Press: Boca Raton, Florida, USA, 1991; Chapter 4.8.

(22) Engel, G. S.; Calhoun, T. R.; Read, E. L.; Ahn, T.-K.; Mančal, T.; Cheng, Y.-C.; Blankenship, R. E.; Fleming, G. R. Evidence for Wavelike Energy Transfer Through Quantum Coherence in Photosynthetic Systems. *Nature* **2007**, *446*, 782−786.

(23) Westenhoff, S.; Paleček, D.; Edlund, P.; Smith, P.; Zigmantas, D. Coherent Picosecond Exciton Dynamics in a Photosynthetic Reaction Center. *J. Am. Chem. Soc.* **2012**, *134*, 16484−16487.

(24) Butkus, V.; Zigmantas, D.; Valkunas, L.; Abramavicius, D. Vibrational vs. Electronic Coherences in 2D Spectrum of Molecular Systems. *Chem. Phys. Lett.* **2012**, *545*, 40−43.

(25) Butkus, V.; Zigmantas, D.; Abramavicius, D.; Valkunas, L. Distinctive Character of Electronic and Vibrational Coherences in Disordered Molecular Aggregates. *Chem. Phys. Lett.* **2013**, *587*, 93−98.

(26) Turner, D. B.; Dinshaw, R.; Lee, K.-K.; Belsley, M. S.; Wilk, K. E.; Curmi, P. M. G.; Scholes, G. D. Quantitative Investigations of Quantum Coherence for a Light-harvesting Protein at Conditions Simulating Photosynthesis. *Phys. Chem. Chem. Phys.* **2012**, *14*, 4857−4874.

(27) Avarmaa, R. A.; Rebane, K. K. High-resolution Optical Spectra of Chlorophyll Molecules. *Spectrochim. Acta, Part A* **1985**, *41*, 1365−1380.

(28) Pieper, J.; Rätsep, M.; Trostmann, I.; Paulsen, H.; Renger, G.; Freiberg, A. Excitonic Energy Level Structure and Pigment-Protein Interactions in the Recombinant Water-Soluble Chlorophyll Protein. I. Difference Fluorescence Line-Narrowing. *J. Phys. Chem. B* **2011**, *115*, 4042−4052.

(29) Christensson, N.; Kauffmann, H. F.; Pullerits, T.; Mančal, T. Origin of Long-Lived Coherences in Light-Harvesting Complexes. *J. Phys. Chem. B* **2012**, *116*, 7449−7454.

(30) Tiwari, V.; Peters, W. K.; Jonas, D. M. Electronic Resonance with Anticorrelated Pigment Vibrations Drives Photosynthetic Energy Transfer Outside the Adiabatic Framework. *Proc. Natl. Acad. Sci. U.S.A.* **2013**, *110*, 1203−1208.
(31) Butkus, V.; Gelzinis, A.; Valkunas, L. Quantum Coherence and Disorder-Specific Effects in Simulations of 2D Optical Spectra of One-Dimensional J-aggregates. *J. Phys. Chem. A* **2011**, *115*, 3876−3885.
(32) Chenu, A.; Christensson, N.; Kauffmann, H. F.; Mančal, T. Enhancement of Vibronic and Ground-State Vibrational Coherences in 2D Spectra of Photosynthetic Complexes. *Sci. Rep.* **2013**, *3*.
(33) Pieper, J.; Rätsep, M.; Trostmann, I.; Schmitt, F. J.; Theiss, C.; Paulsen, H.; Eichler, H. J.; Freiberg, A.; Renger, G. Excitonic Energy Level Structure and Pigment-Protein Interactions in the Recombinant Water-Soluble Chlorophyll Protein. II. Spectral Hole-Burning Experiments. *J. Phys. Chem. B* **2011**, *115*, 4053−4065.